BES-MEMO
Sept. 1996

Measurement of D-meson Production Cross Section in e^+e^- Annihilation at Ec.m.=4.03 GeV

BES Collaboration
Institute of High Energy Physics, Beijing

Abstract

The production cross sections of D-meson are measured with neutral and charged D single tag events based on the data collected by BES detector at a center-of-mass energy 4.03 GeV, corresponding to an integrated luminosity of 22.3 pb^{-1}. D^0 and D^+ reconstructed from decay modes $K^-\pi^+$ and $K^-\pi^+\pi^+$ are used to determine the inclusive production cross sections of neutral and charged D and exclusive cross sections for processes $e^+e^- \to D\bar{D}$, $e^+e^- \to \bar{D}D^*$ or $D\bar{D}^*$, and $e^+e^- \to D^*\bar{D}^*$.

Typeset using REVTEX

I. INTRODUCTION

D-meson production cross section between 3.7-4.3 GeV were predicted by coupled-channel model of charm[1], and were measured mainly by MARK II experiments[2]. More measurements are still required to make a test of this model.

In this paper, we report our measurement results of D-meson production cross section at 4.03 GeV. The analysis is based on $22.3pb^{-1}$ of data from e^+e^- collisions at a centr-of-mass energy 4.03 GeV, taken with the BES detector during the 1992-1994 BEPC run.

The BES is a conventional cylindrical detector, which is described in detail in Ref.[3]. A four-layer central drift chamber (CDC) surrounding the beampipe provides trigger information. Outside the CDC, a forty-layer main drift chamber (MDC) provides tracking and energy loss(dE/dx) information on charged tracks over $\sim$ 85% of the total solid angle. The momentum resolution is $\sigma_p/p = 0.017\sqrt{1+p^2}$ (p in GeV/c), and the energy loss (dE/dx) resolution is $\sim$ 11% for hadron tracks and $\sim$ 8.5% for Bhabha electrons. Scintillation counters which surround the MDC provide time-of-flight (TOF) measurements, with resolutions of $\sim$ 450 ps for hadrons and $\sim$ 330 ps for Bhabha events. Outside the TOF system a 12-radiation-length, lead-gas barrel shower counter (BSC), operating in limited streamer mode, measures the energies of electrons and photons over $\sim$ 80% of the total solid angle,and achieves energy resolution $\sigma_E/E = 0.22/\sqrt{E}$ (E in GeV) for electrons, and spatial resolutions σ_ϕ=4.5 mrad and σ_z=2 cm. A solenoidal magnet provides a 0.4 T magnetic field in the central tracking region of the detector. Three double-layer muon counters (MUC) instrument the magnet flux return, and serve to identify muons of momentum greater than 0.5 GeV/c. They cover $\sim$ 68% of the total solid angle with longitudinal (transverse) spatial resolution of 5 cm (3 cm).

Section II describes the measurement of D-meson production and A brief discussion is presented in Section III.

II. PRODUCTION CROSS SECTION OF D-MESON

In the 4-GeV region, three D production modes have been observed:

(1) $e^+e^- \to D\bar{D}$

(2) $e^+e^- \to D^*\bar{D}$ or $\bar{D}^*D$

(3) $e^+e^- \to D^*\bar{D}^*$

here D and D^* denote charged and neutral D meson and D^* meson respectively. Vector meson D^{*+} may decay to $D^+\gamma$, $D^+\pi^0$ or $D^0\pi^+$; D^{*0} may decay to $D^0\gamma$ or $D^0\pi^0$. Process (1) includes $e^+e^- \to D^0\bar{D}^0$, $e^+e^- \to D^+D^+$; Process (2) includes $e^+e^- \to D^\pm D^{*\mp}$, $e^+e^- \to D^0\bar{D}^{*0}$ or $\bar{D}^0D^{*0}$; Process (3) includes $e^+e^- \to D^{*\pm}D^{*\mp}$, $e^+e^- \to D^{*0}\bar{D}^{*0}$. The momentum regions of D-meson from above production modes are different. We will describe this later.

$D^\pm$, D^0 and $\bar{D}^0$ are reconstructed from the hadronic final states $K^\mp\pi^\pm\pi^\pm$ and $K^\mp\pi^\pm$. Well-reconstructed charged tracks (MFIT=2,-9,-19) were used to combine. Tracks are required to come within 1 cm radialy and within $\pm$15 cm longitudinally of the measured beam crossing point. The polar angle of charged track are required to satisfy $|cos\theta| \leq 0.80$ to provide reliable tracking and barrel TOF information. The dE/dx and TOF information of a charged track are used to identify a particle. They are required to be consistent with the mass hypothesis assigned to the track. The confidence level of a track for each particle hypothesis (e, μ, π, K, P) can be calculated as $CL_i = 1 - Prob(\chi_i^2)$, where $Prob(\chi_i^2)$ is the probability of the χ^2 distribution for each partical hypothesis, $i = e, \mu, \pi, K, P$. χ_i^2 is the joint chi-square of the available dE/dx and TOF information for the track, defined as $\chi_i^2 = \chi_i^2(TOF) + \chi_i^2(dE/dx)$, where $\chi_i^2(TOF) = (t - t_i)^2/\sigma_{TOF}^2$, t is the measured time of flight and t_i is expected time of flight for i particle hypothsis. σ_{TOF}^2 is the resolution of TOF. Samillarly, $\chi_i^2(dE/dx)$ is defined as $\chi_i^2(dE/dx) = (dEdx - dEdX_i)^2/\sigma_{dE/dx}^2$. In event selection, $CL_K > 0.01$ and $L_K/(L_K + L_\pi) > 0.5$ are required for K candidate and $CL_\pi > 0.01$ and $L_K/(L_K + L_\pi) \leq 0.5$ for π candidate, where $L_K = exp(-\chi_K^2(TOF)/2) \cdot exp(-\chi_K^2(dE/dx)/2)$ and $L_\pi = exp(-\chi_\pi^2(TOF)/2) \cdot exp(-\chi_\pi^2(dE/dx)/2)$. Further more, measured momenta of track are corrected for dE/dx losses in material traversed, and for a shift of BES magnetic field.

Signals of $D^\pm$, D^0 and $\bar{D}^0$ are observed. Fig.1 shows the invariant mass distributions of $K^\mp\pi^\pm$, $K^\mp\pi^\pm\pi^\pm$. Fig.2 shows the momenta distribution of $K^\mp\pi^\pm$ and $K^\mp\pi^\pm\pi^\pm$ under a cut of $|M_{K\pi} - 1.865| \leq 0.05$ GeV and $|M_{K\pi\pi} - 1.869| \leq 0.05$ GeV respectively. Momenta regions for production mode (1), (2), (3) seperate well. They are listed in Table I. So, one can determine from which production mode a reconstructed D-meson comes by the momentum of D.

The ammounts of tagged $D^\pm$, D^0 and $\bar{D}^0$ can be determined by fitting the invariant-mass distributions to Breit-Weigner function. The mean value of mass and width(σ) are obtained, as listed in Table II. Numbers of tagged $D^\pm$, $D^0(\bar{D}^0)$ produced from each production mode, as listed in Table III, are determined by fitting the inariant-mass distribution under cuts on momentum, see Fig.3.

In order to perform the calculation of cross section, efficences of reconstruction via $K^-\pi^+\pi^+$ and $K^-\pi^+$ for each event type are determined by Monte Carlo studies. There are eight event types for D^0 and six types for D^+ in the production at Ecm=4.03 GeV. We generated Monte Carlo events in the way that one side, i.e. one determined D, decays to indicated chennal whereas, the other side decays to cocktail. Efficiences for each event type are obtained, as listed in Table IV.

We denote $br^+ = BR(D^+ \to K^-\pi^+\pi^+)$, $br^0 = BR(D^0 \to K^-\pi^+)$, $b_1 = BR(D^{*+} \to D^+\gamma)$, $b_2 = BR(D^{*+} \to D^+\pi^0)$, $b_3 = BR(D^{*+} \to D^0\pi^+)$, $b_1^0 = BR(D^{*0} \to D^0\gamma)$ and $b_2^0 = BR(D^{*0} \to D^0\pi^0)$. From Ref.[4], we have $br^+ = 9.1 \pm 0.6\%$, $br^0 = 4.01 \pm 0.14\%$, $b_1 = 1.1 \pm 0.6\%$, $b_2 = 30.8 \pm 0.8\%$, $b_3 = 68.1 \pm 1.3\%$, $b_1^0 = 36.4 \pm 2.8\%$ and $b_1^0 = 63.6 \pm 2.8\%$.

In the determining of cross sections, contributions of revalent event type are considered. In the process of $e^+e^- \to D\bar{D}$, the numbers of tagged D^+ and D^0 can be written as follows:

$$N_{D^0} = L \cdot \sigma(D^0\bar{D}^0) \cdot \varepsilon_1^0 \cdot br^0 \tag{1}$$

$$N_{D^+} = L \cdot \sigma(D^+D^-) \cdot \varepsilon_1 \cdot br^+ \tag{2}$$

where the integreted luminosity $L = 22.3\ pb^{-1}$. $\sigma(D^+D^-)$ and $\sigma(D^0\bar{D}^0)$ are the exclusive production cross sections of $e^+e^- \to D^+D^-$ and $e^+e^- \to D^0\bar{D}^0$ respectively. ε_1 and ε_1^0 are efficiencies of associated event type, whose values are listed in Table IV. The inclusive production cross section of D^+ and D^0 come from this mode can be calculated as

$$\sigma(D^0) = \sigma(D^0\bar{D}^0) \tag{3}$$

$$\sigma(D^+) = \sigma(D^+D^-). \tag{4}$$

In the process of $e^+e^- \to DD^*$ or $\bar{D}D^*$, we have

$$N_{D^+} = L \cdot \sigma(D^+D^{*-}) \cdot (\varepsilon_2 + \varepsilon_3 \cdot b_1 + \varepsilon_4 \cdot b_2) \cdot br^+ \tag{5}$$

$$N_{D^0} = L \cdot \sigma(D^0\bar{D}^{*0}) \cdot (\varepsilon_2^0 + \varepsilon_3^0 \cdot b_1^0 + \varepsilon_4^0 \cdot b_2^0) \cdot br^0 + L \cdot \sigma(D^+D^{*-}) \cdot \varepsilon_5^0 \cdot b_3 \cdot br^0 \tag{6}$$

and then there are

$$\sigma(D^+) = (1 + b_1 + b_2) \cdot \sigma(D^+D^{*-}) \tag{7}$$

$$\sigma(D^0) = b_3 \cdot \sigma(D^+D^{*-}) + 2 \cdot \sigma(D^0\bar{D}^{*0}) \tag{8}$$

In the process of $e^+e^- \to D^*\bar{D}^*$, we have

$$N_{D^+} = L \cdot \sigma(D^{*+}D^{*-}) \cdot (\varepsilon_5 \cdot b_1 + \varepsilon_6 \cdot b_2) \cdot br^+ \tag{9}$$

$$N_{D^0} = L \cdot \sigma(\bar{D}^{*0}D^{*0}) \cdot (\varepsilon_6^0 \cdot b_1^0 + \varepsilon_7^0 \cdot b_2^0) \cdot br^0 + L \cdot \sigma(D^{*+}D^{*-}) \cdot \varepsilon_8^0 \cdot b_3 \cdot br^0 \tag{10}$$

then we get

$$\sigma(D^+) = (b_1 + b_2) \cdot \sigma(D^{*+}D^{*-}) \tag{11}$$

$$\sigma(D^0) = \sigma(D^{*0}\bar{D}^{*0}) + b_3 \cdot \sigma(D^{*+}D^{*-}) \tag{12}$$

By Substituting the values of numbers of single tagged D^+ and D^0 (becaues of charge conjugation, $N_{D^+} = N_{D^\pm}/2$, and similarly for N_{D^0}) for each production mode, branching fraction values and efficiencies for each event type, cross sections can be obtained from a calculation performance. We list the results in Table V and Table VI. The first item of error is statistic error caused by statistic uncertainty of ΔN_D. The second item of error is systematic error due to the uncertainty of br^+ and br^0, a variation of luminosity L by 2.5% and the uncertainty of N_D via varying background function used in mass fitting. The systematic error caused by a variation of efficiences are not included. A variation of average efficiences by 10% will cause a change of inclusive D cross section by 10%.

III. DISCUSSION

Coupled-channel model[1] predicts the rate of charm production cross sections at $\Psi(4028)$ to be:
$R_{(D^{*0}\bar{D}^{*0})} : R_{(D^0\bar{D}^{*0}+\bar{D}^0D^{*0})} : R_{(D^0\bar{D}^0)} = 1.0 : 1.35 : 0.005$
$R_{(D^{*+}D^{*-})} : R_{(D^+D^{*-}+D^-D^{*+})} : R_{(D^+D^-)} = 1.0 : 2.69 : 0.004$

SLAC-LBL gave a measurement at $\Psi(4028)$ that:
$R_{(D^{*0}\bar{D}^{*0})} : R_{(D^0\bar{D}^{*0}+\bar{D}^0D^{*0})} : R_{(D^0\bar{D}^0)} = (1.0 \pm 0.10) : (0.85 \pm 0.09) : (0.10 \pm 0.06)$
The rates of charged D cross sections were not given.

In this experiment, we can give these rates as follows:
$R_{(D^{*0}\bar{D}^{*0})} : R_{(D^0\bar{D}^{*0}+\bar{D}^0D^{*0})} : R_{(D^0\bar{D}^0)} = (1.00 \pm 0.13) : (1.35 \pm 0.23) : (0.07 \pm 0.02)$
$R_{(D^{*+}D^{*-})} : R_{(D^+D^{*-}+D^-D^{*+})} : R_{(D^+D^-)} = (1.00 \pm 0.14) : (2.20 \pm 0.18) : (0.08 - 0.08)$
We find the rate of netral D are in good agreement with coupled-channel model whereas, rate of charged D has small difference.

We would like to thank the staffs of the BEPC accelerator and the Computing Center at the Institute of High Energy Physics (Beijing).

REFERENCES

[1] E. Eichten *et.al.*, Phys. Rev. D **21**, 227 (1980); E. Eichten *et.al.*, Phys. Rev. D **17**, 3090 (1978).

[2] G.Goldhaber *et. al.*, Phys. Lett. **69B**, 503 (1977); MarK II Collaboration, M. W. Coles *et. al.*, Phys. Rev. D **26**, 2190 (1982).

[3] J. Z. Bai *et al.*, Nucl. Instr. and Methods **A344**, 319 (1994); J. Z. Bai *et al.*, Phys. Rev. Lett. **69**, 3021 (1992);

[4] Particle Dara Group, Phys. Rev. D **50**, 1173 (1994).

TABLES

TABLE I. Momenta range for production modes

production mode	theoreticl momenta	experimental momenta
$e^+e^- \to D^*\bar{D}^*$	0.004-0.308 GeV	0.0-0.34 GeV
$e^+e^- \to D^*\bar{D}$ or $\bar{D}^*D$	0.368-0.664 GeV	0.34-0.70 GeV
$e^+e^- \to D\bar{D}$	P_{D^+}:0.752, P_{D^0}:0.764 GeV	0.70-0.85 GeV

TABLE II. Event number and mass for each tag Channel

Channel	mass(GeV)	width(MeV)
$D^0 \to K^-\pi^+$	1.8659±0.0007	27.6 ± 0.9
$D^+ \to K^-\pi^+\pi^+$	1.8683±0.0009	21.0 ± 1.0

TABLE III. Events number for each production mode ($P_D : GeV$)

		event number N_D		
Channel	$e^+e^- \to D^*\bar{D}^*$	$e^+e^- \to D^*\bar{D}(\bar{D}^*D)$	$e^+e^- \to D\bar{D}$	total
	$p_D < 0.34$	$0.34 < P_D < 0.70$	$0.70 < P_D < 0.85$	
$D^0 \to K^-\pi^+$	$1809 \pm 63 \pm 53$	$2090 \pm 110 \pm 107$	82 ± 28	$3899 \pm 127 \pm 119$
$D^+ \to K^-\pi^+\pi^+$	$428 \pm 43 \pm 7$	$1722 \pm 77 \pm 9$	< 95	$2150 \pm 88 \pm 11$

TABLE IV. Efficence for each event type

event type	efficiency (%)
$e^+e^- \to D^+D^-, directD$	$\varepsilon_1 = 0.289$
$e^+e^- \to D^+D^{*-}, directD$	$\varepsilon_2 = 0.265$
$e^+e^- \to D^-D^{*+}, D^{*+} \to D^+\gamma$	$\varepsilon_3 = 0.302$
$e^+e^- \to D^-D^{*+}, D^{*+} \to D^+\pi^0$	$\varepsilon_4 = 0.308$
$e^+e^- \to D^{*-}D^{*+}, D^{*+} \to D^+\gamma$	$\varepsilon_5 = 0.295$
$e^+e^- \to D^{*-}D^{*+}, D^{*+} \to D^+\pi^0$	$\varepsilon_6 = 0.312$
$e^+e^- \to D^0\bar{D}^0, directD^0$	$\varepsilon_1^0 = 0.354$
$e^+e^- \to D^0\bar{D}^{*0}, directD^0$	$\varepsilon_2^0 = 0.344$
$e^+e^- \to \bar{D}^0D^{*0}, D^{*0} \to D^0\gamma$	$\varepsilon_3^0 = 0.371$
$e^+e^- \to \bar{D}^0D^{*0}, D^{*0} \to D^0\pi^0$	$\varepsilon_4^0 = 0.375$
$e^+e^- \to D^-D^{*+}, D^{*+} \to D^0\pi^+$	$\varepsilon_5^0 = 0.357$
$e^+e^- \to \bar{D}^{*0}D^{*0}, D^{*0} \to D^0\gamma$	$\varepsilon_6^0 = 0.387$
$e^+e^- \to \bar{D}^{*0}D^{*0}, D^{*0} \to D^0\pi^0$	$\varepsilon_7^0 = 0.403$
$e^+e^- \to D^{*-}D^{*+}, D^{*+} \to D^0\pi^+$	$\varepsilon_8^0 = 0.394$

TABLE V. Inclusive production cross sections of D^+ and D^0 (charge conjugation included)

production mode	$\sigma(D^0)$	$\sigma(D^+)$
$e^+e^- \to D^*\bar{D}^*$	$5.11 \pm 0.27 \pm 0.44$ nb	$0.68 \pm 0.07 \pm 0.07$ nb
$e^+e^- \to D\bar{D}^*$	$6.52 \pm 0.36 \pm 0.80$ nb	$3.09 \pm 0.14 \pm 0.22$ nb
$e^+e^- \to D\bar{D}$	0.26 ± 0.09 nb	< 0.16 nb
Total(exclude $D\bar{D}$)	$11.63 \pm 0.45 \pm 0.91$ nb	$3.77 \pm 0.15 \pm 0.23$ nb

TABLE VI. Exclusive production cross section for each mode

production mode	cross section
$e^+e^- \to D^{*+}D^{*-}$	$\sigma(D^{*+}D^{*-}) = 1.06 \pm 0.11 \pm 0.10$ nb
$e^+e^- \to D^{*0}\bar{D}^{*0}$	$\sigma(D^{*0}\bar{D}^{*0}) = 1.83 \pm 0.12 \pm 0.21$ nb
$e^+e^- \to D^{\pm}D^{*\mp}$	$\sigma(D^{\pm}D^{*\mp}) = 2.34 \pm 0.10 \pm 0.17$ nb
$e^+e^- \to \bar{D}^0D^{*0}$ or $D^0\bar{D}^{*0}$	$\sigma(\bar{D}^0D^{*0}$ & $D^0\bar{D}^{*0}) = 2.46 \pm 0.18 \pm 0.39$ nb
$e^+e^- \to D^+D^-$	$\sigma(D^+D^-) \leq 0.08$ nb
$e^+e^- \to D^0\bar{D}^0$	$\sigma(D^0\bar{D}^0) = 0.13 \pm 0.04$ nb

FIGURES

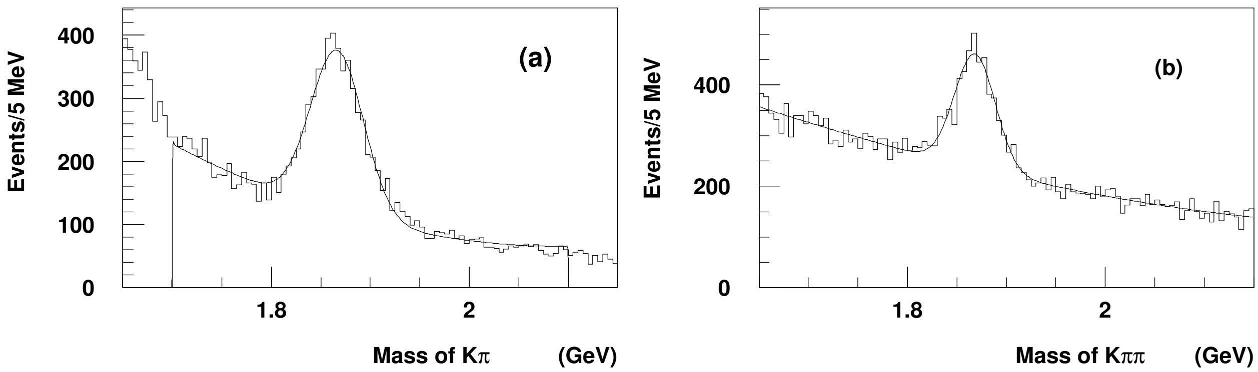

FIG. 1. Invariarant mass distribution for (a). $D^0 \to K^- \pi^+$, (b). $D^+ \to K^- \pi^+ \pi^+$

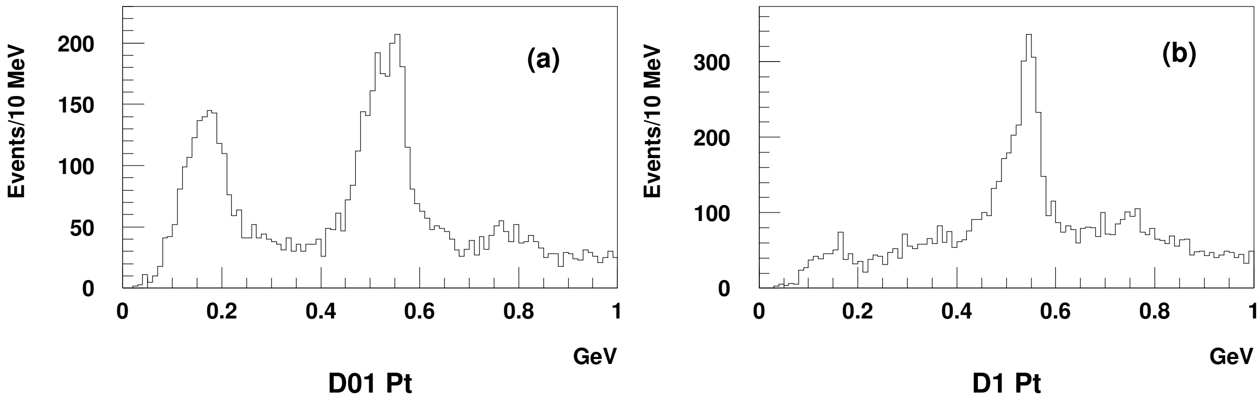

FIG. 2. Momenta distribution for (a). $D^0 \to K^- \pi^+$ and (b). $D^+ \to K^- \pi^+ \pi^+$

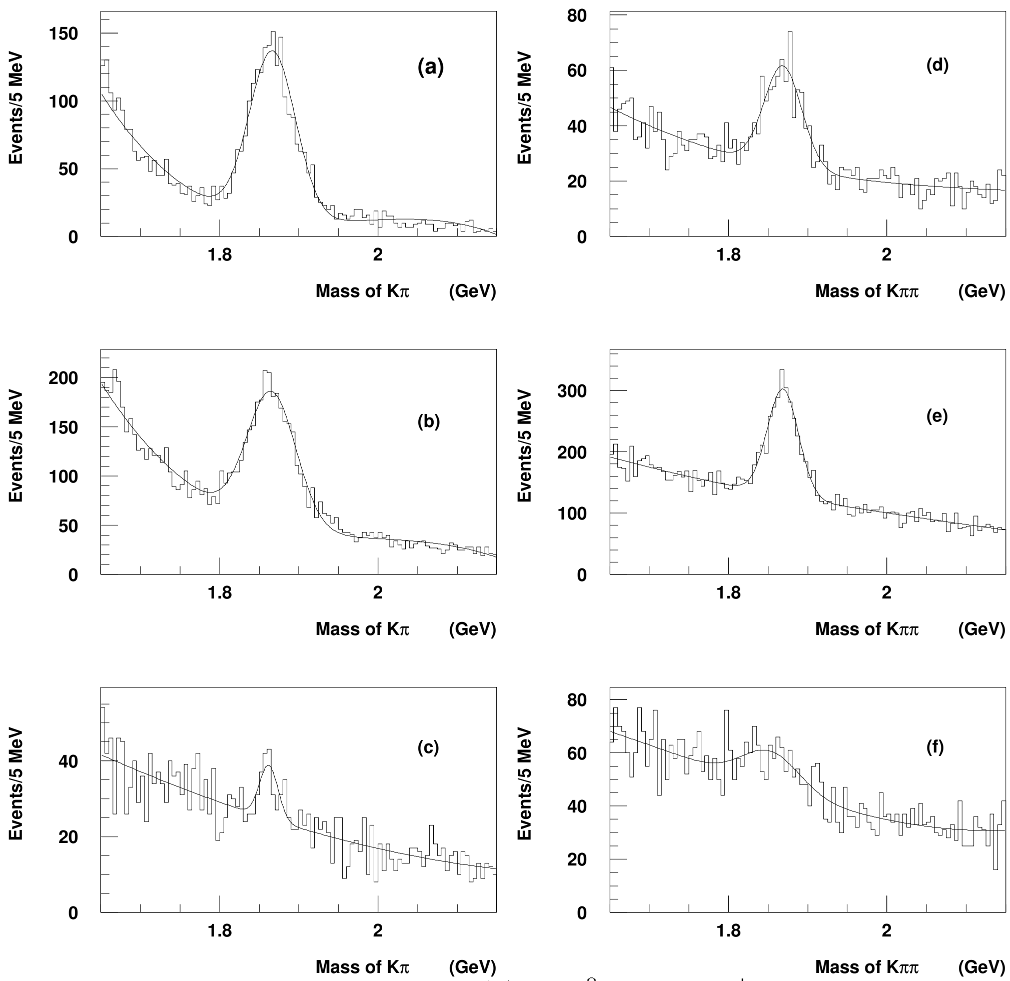

FIG. 3. Invariarant mass distribution. (a). $D^0 \rightarrow K^-\pi^+$, with P $<$ 0.34 GeV. (b). $D^0 \rightarrow K^-\pi^+$, with 0.34 GeV $\leq$ P $<$ 0.70 GeV. (c). $D^0 \rightarrow K^-\pi^+$, with 0.70 GeV $\leq$ P $<$ 0.85 GeV. (d). $D^+ \rightarrow K^-\pi^+\pi^+$, with P $<$ 0.34 GeV. (e). $D^+ \rightarrow K^-\pi^+\pi^+$, with 0.34 GeV $\leq$ P $<$ 0.70 GeV. (f). $D^+ \rightarrow K^-\pi^+\pi^+$, with 0.70 GeV $\leq$ P $<$ 0.85 GeV.